J. Fluid Mech. (1981), *vol.* 107, *pp.* 423–439
Printed in Great Britain

Velocity redistribution in curved rectangular channels

By H. J. DE VRIEND

Department of Civil Engineering, Delft University of Technology,
The Netherlands

(Received 25 February 1980 and in revised form 10 September 1980)

The main velocity redistribution in steady flow through curved conduits of shallow rectangular cross-section is considered. Its mechanism is analysed using a mathematical model of steady incompressible laminar flow in coiled rectangular pipes. The transverse transport of main-flow momentum by the secondary circulation is shown to be the principal cause of this velocity redistribution. The importance of the side-wall regions, even in shallow channels, is assessed and the neglect of the influence of the side walls in the commonly applied simplified models of flow through shallow curved channels is shown to be strongly limiting in case of long bends with a rectangular cross-section.

1. Introduction

Curved conduit flows are encountered in many engineering problems, from heat exchangers to meandering rivers. Until some ten years ago, these flows could hardly be predicted mathematically. Only specific classes of problems allow for an analytical solution (Dean 1928*a*; Adler 1934; Itō 1951) and otherwise only certain aspects of the flow, such as the secondary circulation in shallow channels far from the side walls, can be treated without computer (Boussinesq 1868 and many others afterwards). Recent advances in computational fluid dynamics, however, have opened the way to fully three-dimensional computations of this type of flow (Patankar, Pratap & Spalding 1974, 1975; Leschziner & Rodi 1978). This provides the possibility of detailed and accurate flow predictions, but also of a thorough analysis. Hitherto, predictions have been extensively reported in the literature, but little attention has yet been paid to analysis. Still such an analysis can be important, especially when it is necessary to simplify the mathematical description of this complex flow. This need of simplification is felt in river engineering, for instance, where the mathematical prediction of flow and bed topography in alluvial river bends requires multiply repeated flow computations with continually changing bottom configurations, so that a fully three-dimensional flow model would become too expensive. Introducing simplifications in the mathematical model, however, requires a proper understanding of the essential phenomena and an analysis of the flow is indispensable then.

The most striking feature of curved conduit flow, the secondary circulation, has been amply considered in the literature (Rozovskii 1961) and it seems to be properly understood, at least qualitatively. The existing analyses of the systematic deformation of the main velocity distribution in a bend, however, give less satisfactory results, mainly because they are based on oversimplified descriptions of the flow, e.g. potential flow (Böss 1938; Kamiyama 1966); wall-layer approximation (Einstein & Harder

1954; Muramoto 1965); shallow-channel approximations (Van Bendegom 1947; Rozovskii 1961; De Vriend 1976; Falcón 1979; and many others). Furthermore, a most important cause of main velocity redistribution, the convective transport of main flow momentum by the secondary flow, is often disregarded or inappropriately incorporated. The present analysis of the main velocity redistribution in curved shallow channels is carried out using a mathematical model of fully developed laminar flow in curved rectangular pipes. In view of the relevance to river engineering suggested before, this approach may seem rather inappropriate; in river bends the flow is turbulent, it often does not reach its fully developed curved stage, natural river channels are not rectangular and the water surface is free.

The differences between laminar and turbulent flow are obvious. They make it impossible to describe the time-mean velocities and pressures by the same mathematical system as in case of laminar flow. Still there are points of qualitative resemblance between the two flow types. Firstly, in many turbulent flows the net convective exchange of momentum due to the velocity fluctuations can be modelled on the analogy of molecular diffusion (Boussinesq hypothesis). The coefficient of turbulent diffusivity (turbulence viscosity) in such models, though varying over the flow field, qualitatively corresponds with the molecular viscosity. Although it must be doubted whether the Boussinesq hypothesis is valid for every detail of turbulent flow in curved ducts, mathematical models using a turbulence viscosity have been shown to yield good predictions of the main velocity distribution in that case (Pratap & Spalding 1975; Leschziner & Rodi 1978). In addition, both laminar and turbulent flow in curved conduits show the characteristic helical flow pattern, caused by the same mechanism in either case. Besides, the redistribution of the main velocity along a bend shows the same features for laminar and turbulent flow (cf. Patankar *et al.* 1974, 1975). In view of these points of resemblance it seems justifiable to utilize a mathematical model of laminar flow for a qualitative analysis of the mechanism of main velocity redistribution in bends, both for laminar and for turbulent flow, provided that the Reynolds number in case of turbulent flow is based on a characteristic value of the turbulence viscosity rather than on the molecular viscosity.

The main flow in river bends seldomly reaches its fully developed stage and, if it does so, it will be only in the last part of a long bend (Muramoto 1965). Hence a mathematical model of fully developed curved flow is definitely unsuited to a description of the flow in a river bend. On the other hand, the convective influence of the secondary flow on the main velocity takes place in cross-stream planes and the streamwise variations of the main flow are not likely to play an important role in it. Therefore a fully developed flow model can be utilized to analyse the mechanism of this influencing.

The cross-sectional shape of curved alluvial river channels is far from rectangular, with a mildly sloping point bar in the inner part of the bend and a scour hole in the outer part, which gives rise to a rather steep concave bank. On the other hand, most laboratory experiments on the flow and the bottom configuration in river bends have been carried out in flumes with vertical sidewalls and it will be shown hereafter that for a proper interpretation of the measured data the effect of these vertical walls on the flow must be taken into account. Therefore the present analysis is made for rectangular channels and an attempt will be made to transfer the conclusions to channels of a more natural shape.

For the flows to be considered here the Froude number is rather small. This implies

that the free water surface can be approximated as a frictionless flat plate (rigid-lid approximation; cf. Leschziner & Rodi 1978), so that in case of a rectangular channel the surface is a plane of symmetry parallel to the bottom. Then the velocity field is the same as in the lower half of a rectangular pipe with a height of twice the channel depth.

Although it may be evident that a mathematical model of fully developed laminar flow in curved rectangular ducts cannot serve as a model of the flow in river bends, the foregoing arguments justify a qualitative analysis of the mechanism of main velocity redistribution due to the secondary flow in curved channels on the basis of this relatively simple and well-documented flow case. This flow case allows for the numerical solution of the complete steady-state Navier–Stokes equations without extremely high computer costs. Hence it is possible to investigate the influence of the various physical phenomena involved by manipulating the relevant terms in the equations (cf. Humphrey, Taylor & Whitelaw 1977).

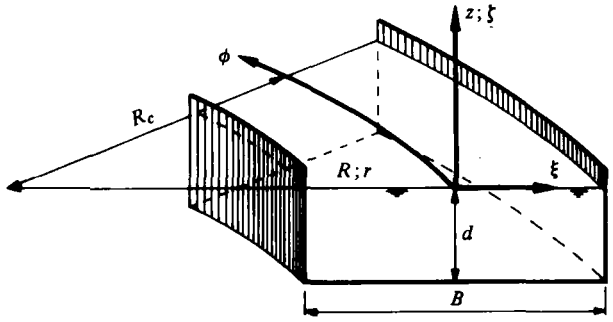

FIGURE 1. Definition sketch.

2. Mathematical model

For the mathematical description of the flow situation to be considered (figure 1) a cylindrical co-ordinate system (R, ϕ, z) is adopted, with the z axis through the centre of curvature of the channel axis and directed vertically upwards. Then the velocity components, v_R, v_ϕ and v_z and the pressure p are described by a system of four differential equations representing the conservation of mass and R, ϕ and z momentum, with an appropriate set of boundary conditions. After the normalization

$$v_\phi = Vu, \quad v_R = \delta V v, \quad v_z = \delta V w, \quad p + \rho g z = \frac{\rho V^2}{Re}\tilde{p}, \tag{1}$$

$$\frac{\partial}{\partial R} = \frac{1}{d}\frac{\partial}{\partial \xi} \quad \text{with} \quad \xi = \frac{R - R_c}{d}, \quad \frac{1}{R}\frac{\partial}{\partial \phi} = \frac{1}{R_c}\frac{1}{r}\frac{\partial}{\partial \phi}, \quad \frac{\partial}{\partial z} = \frac{1}{d}\frac{\partial}{\partial \zeta}, \quad \frac{1}{R} = \frac{1}{R_c}\frac{1}{r} \tag{2}$$

(V = overall mean velocity, δ = curvature ratio d/R_c, d = mean depth of flow, R_c = radius of the channel axis, ρ = mass density of the fluid, g = acceleration due to gravity, Re = Reynolds number Vd/ν, ν = kinematic viscosity of the fluid), this system of equations reads

$$\frac{1}{r}\frac{\partial u}{\partial \phi} = 0 \quad \text{and} \quad \frac{\partial v}{\partial \xi} + \frac{\delta}{r}v + \frac{\partial w}{\partial \zeta} = 0, \tag{3}$$

$$\delta Re\left(v\frac{\partial u}{\partial \xi}+w\frac{\partial u}{\partial \zeta}+\frac{\delta}{r}uv\right)=-\frac{\delta}{r}\frac{\partial \tilde{p}}{\partial \phi}+\nabla^2 u-\frac{\delta^2}{r^2}u, \tag{4}$$

$$\delta^2 Re\left(v\frac{\partial v}{\partial \xi}+w\frac{\partial v}{\partial \zeta}\right)-\delta Re\frac{u^2}{r}=-\frac{\partial \tilde{p}}{\partial \xi}+\delta\nabla^2 v-\frac{\delta^3}{r^2}v, \tag{5}$$

$$\delta^2 Re\left(v\frac{\partial w}{\partial \xi}+w\frac{\partial w}{\partial \zeta}\right)=-\frac{\partial \tilde{p}}{\partial \zeta}+\delta\nabla^2 w, \tag{6}$$

with $$\nabla^2=\frac{\partial^2}{\partial \zeta^2}+\frac{\partial^2}{\partial \xi^2}+\frac{\delta}{r}\frac{\partial}{\partial \xi}.$$

The boundary conditions at the (horizontal) bottom and at the vertical side walls are

$$u=0,\quad v=0,\quad w=0\quad \text{at}\quad \zeta=-1\quad \text{and at}\quad \xi=\pm\frac{B}{2d} \tag{7}$$

(B = channel width). The water surface is approximated by a rigid frictionless plate parallel to the bottom, so that it is equivalent to the horizontal plane of symmetry in a pipe of height $2d$. The relevant boundary conditions are

$$\frac{\partial u}{\partial \zeta}=0,\quad \frac{\partial v}{\partial \zeta}=0,\quad w=0\quad \text{at}\quad \zeta=0. \tag{8}$$

Although the system (3)–(8) can be solved in this form (Joseph, Smith & Adler 1975), the radial and vertical momentum equations and the equation of continuity for the secondary flow will be reformulated in terms of a stream function in order to reduce the number of equations to be solved simultaneously. As becomes evident from equations (5) and (6), the combination of radial pressure gradients and centripetal accelerations is the only source of secondary flow. As this source is almost proportional to Re, the stream function of the secondary flow is defined by

$$v=-\frac{Re}{r}\frac{\partial \psi}{\partial \zeta},\quad w=\frac{Re}{r}\frac{\partial \psi}{\partial \xi}. \tag{9}$$

Thus the equation of continuity for the secondary flow is satisfied and the momentum equations (5) and (6) can be rewritten, in terms of ψ and the secondary-flow vorticity $\omega=\partial w/\partial \xi-\partial v/\partial \zeta$,

$$\delta Re^2\left\{-\frac{1}{r}\frac{\partial \psi}{\partial \zeta}\left(\frac{\partial \omega}{\partial \xi}-\frac{\delta}{r}\omega\right)+\frac{1}{r}\frac{\partial \psi}{\partial \xi}\frac{\partial \omega}{\partial \zeta}\right\}+Re\frac{\partial}{\partial \zeta}\left(\frac{u^2}{r}\right)=\nabla^2\omega, \tag{10}$$

whereas the definition of ω can be elaborated to

$$\omega=Re\left(\frac{1}{r}\nabla^2\psi-\frac{\delta}{r^2}\frac{\partial \psi}{\partial \xi}\right). \tag{11}$$

The boundary conditions for v and w lead to

$$\psi=0,\quad \frac{\partial \psi}{\partial \zeta}=0\quad \text{at}\quad \zeta=-1;\quad \psi=0,\quad \frac{\partial \psi}{\partial \xi}=0\quad \text{at}\quad \xi=\pm\frac{B}{2d}; \tag{12}$$

$$\psi=0,\quad \frac{\partial^2\psi}{\partial \zeta^2}=0\quad \text{at}\quad \zeta=0. \tag{13}$$

The longitudinal momentum equation (4) then becomes

$$\delta Re^2\left\{-\frac{1}{r}\frac{\partial \psi}{\partial \zeta}\left(\frac{\partial u}{\partial \xi}+\frac{\delta}{r}u\right)+\frac{1}{r}\frac{\partial \psi}{\partial \xi}\frac{\partial u}{\partial \zeta}\right\}=\frac{\delta}{r}i+\nabla^2 u-\frac{\delta^2}{r^2}u, \tag{14}$$

where $i = -\partial\tilde{p}/\partial\phi$ is a constant to be determined from the integral condition of continuity

$$\int_{-B/2d}^{B/2d} d\xi \int_{-1}^{0} u\, d\zeta = \frac{B}{d}. \tag{15}$$

The system (10)–(15) with the boundary conditions

$$u = 0 \quad \text{at} \quad \zeta = -1 \quad \text{and} \quad \frac{\partial u}{\partial \zeta} = 0 \quad \text{at} \quad \zeta = 0 \tag{16}$$

can be solved by an iterative procedure (Cheng, Lin & Ou 1976). In the present model the number of equations is further reduced by combining equations (10) and (11) to one fourth-order equation for ψ (see also Cheng & Akiyama 1970). Thus the problem of the boundary conditions for ω (Roache 1972) is avoided.

Once u, ω and ψ are known, the pressure follows from

$$\nabla^2\left(\tilde{p} + \delta^2 Re\,\frac{v^2+w^2}{2}\right) = \delta^2 Re\left\{w\left(\frac{\partial\omega}{\partial\xi} + \frac{\delta}{r}\,\omega\right) - v\,\frac{\partial\omega}{\partial\zeta} + \omega^2\right\} + \frac{\delta Re}{r}\,\frac{\partial u^2}{\partial\xi} \tag{17}$$

with the boundary conditions

$$\frac{\partial\tilde{p}}{\partial\xi} = \delta\,\frac{\partial^2 v}{\partial\zeta^2} \quad \text{at} \quad \zeta = -1; \quad \frac{\partial\tilde{p}}{\partial\zeta} = \delta\left(\frac{\partial^2 w}{\partial\zeta^2} + \frac{\delta}{r}\,\frac{\partial w}{\partial\xi}\right) \quad \text{at} \quad \xi = \pm\frac{B}{2d}; \tag{18}$$

$$\frac{\partial\tilde{p}}{\partial\zeta} = 0 \quad \text{at} \quad \zeta = 0. \tag{19}$$

Numerical details of the solution procedure of the system (10)–(19) will not be given here, all elements being well known. Besides, equivalent or even more extensively applicable mathematical models have been described before (Cheng & Akiyama 1970; J oseph *et al.* 1975; Cheng *et al.* 1976; see also Collins & Dennis 1975, 1976).

For the same reason it may suffice here to state that the model was verified in three different ways, viz.:

(i) by comparing its result for small values of the Dean number $De = Re\,\delta^{\frac{1}{2}}$ with analytical solutions given by Itō (1951), Cuming (1952) and De Vriend (1973);

(ii) by comparing its results with those from the other numerical models mentioned before;

(iii) by comparing its results with measured data given by Mori, Uchida & Ukon (1971).

It became evident from these comparisons that for Dean numbers up to about 60 the model gives a good description of fully developed laminar flow in curved conduits with a rectangular cross-section of aspect ratio $d/B < 0{\cdot}5$. For further details of this verification, see De Vriend (1978).

It should be noted that the mathematical model described here is in general inferior to models solving equations (10) and (11) instead of the fourth-order equation for ψ, in so far that convergence is limited to much smaller values of the Dean number (see, for instance, Cheng *et al.* 1976; also Collins & Dennis 1975, 1976). The present investigations, however, are not aiming at the development of an efficient and sophisticated mathematical model of fully developed curved laminar flow, but rather at the analysis of the main velocity redistribution in a channel bend. From that point of view, the present model is also acceptable, at least within its range of validity ($De < 60$). The

range of effective Dean numbers in meandering rivers can be estimated as follows. Engelund (1974) states that the mean turbulence viscosity in such rivers is approximately equal to $0{\cdot}077V_* d$, where V_* denotes the mean wall friction velocity. Hence the effective Reynolds number can be taken $13V/V_*$, which varies in practice between 100 and 250. According to Leopold, Wolman & Miller (1964), the ratio R_c/B for meandering natural rivers ranges from 2 to 3, so that for channels with $d/B < 0{\cdot}1$ the effective Dean number ranges up to about 55. With some reserve as to the equivalence of the Dean number for laminar flow and the effective Dean number for turbulent flow, it can be concluded that the present model qualitatively covers the greater part of turbulent flows in natural river bends.

3. Main velocity redistribution

The longitudinal momentum equation (14) differs from its straight channel equivalent

$$0 = \delta i + \nabla_0^2 u, \quad \nabla_0^2 = \frac{\partial^2}{\partial \zeta^2} + \frac{\partial^2}{\partial \xi^2} \tag{20}$$

at the following points:

(i) the factor $1/r$ in the longitudinal pressure gradient term,

(ii) the extra diffusion terms arising from the curvature of the co-ordinate system,

(iii) the convection terms.

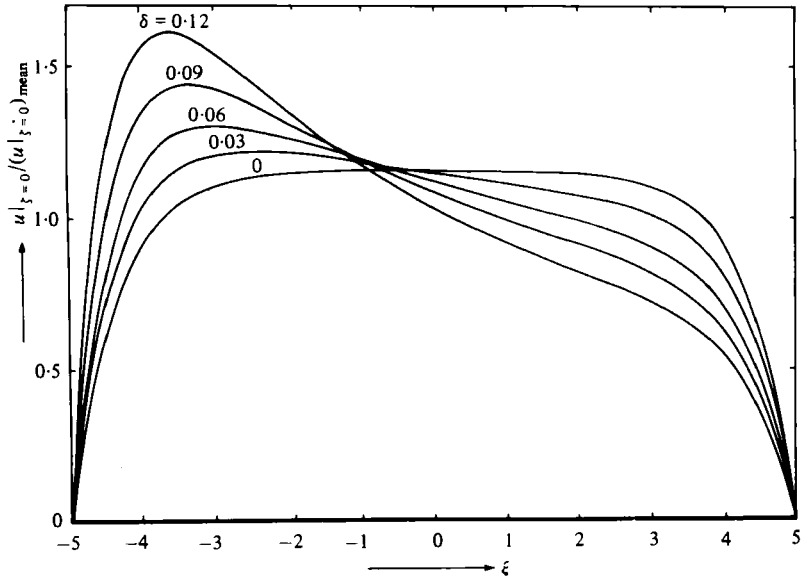

FIGURE 2. Potential flow effect.

Each of these differences causes deformations of the main velocity distribution with respect to its straight channel shape. The combination of the first two differences gives rise to what is called the potential flow effect: the velocity distribution is skewed inwards and away from the side walls it approaches the free-vortex distribution (see figure 2). The convection terms, the importance of which is indicated by the square of the Dean number, act in an opposite sense: the main velocity distribution tends to

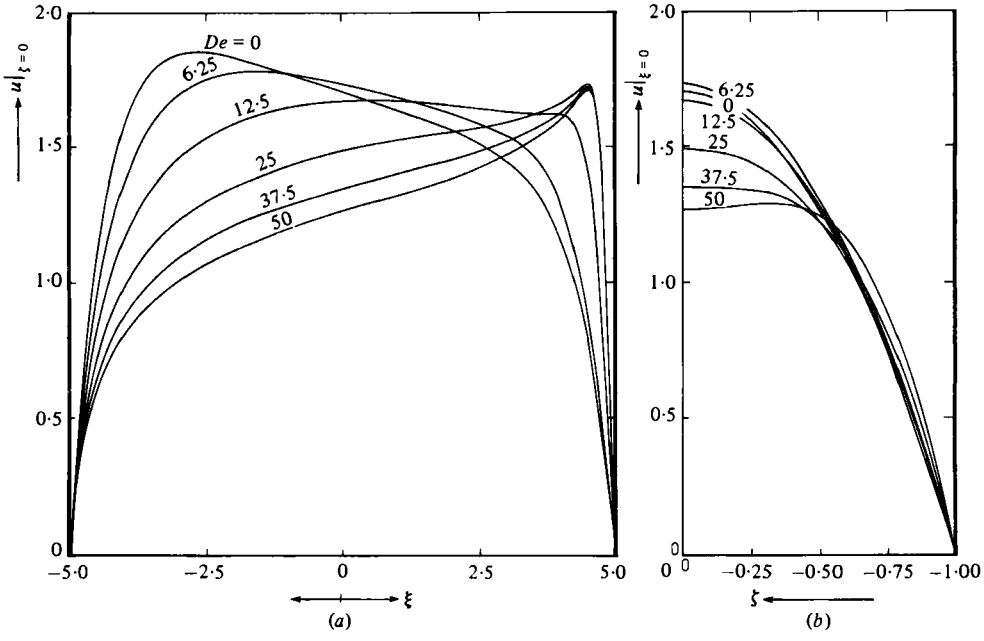

FIGURE 3. Influence of the Dean number on the main velocity distribution in a shallow channel. (*a*) At the surface; (*b*) in the centre-line.

be skewed as De increases (figure 3*a*). In addition, the vertical distribution becomes flatter and at higher De the velocity maximum even lies below the surface (figure 3*b*). The mechanism of the convective redistribution of the main velocity will be analysed further, making use of the mathematical model described in § 2. With a view to the mathematical modelling of curved shallow channel flow, the influence of the various terms in the longitudinal momentum equation will be investigated and a physical interpretation of the observed phenomena will be given.

4. Analysis for low-Dean-number flow

Low-Dean-number flow is suited for a first analysis of the convective redistribution of the main velocity, since it allows for a relatively simple mathematical approach in the form of perturbations of the zero-Dean-number solution with De^2 as a perturbation parameter. Hence

$$u = \sum_{k=0}^{\infty} De^{2k} u_k; \quad i = \sum_{k=0}^{\infty} De^{2k} i_k; \quad \psi = \sum_{k=0}^{\infty} De^{2k} \psi_k. \tag{21}$$

If lateral diffusion is neglected, the first two terms of the series for u are (cf. De Vriend 1971)

$$u = (\bar{u}_0 + De^2 \bar{u}_1)[\tfrac{3}{2}(1-\zeta^2)] + De^2 \left\{ \frac{\bar{\psi}_0}{r} \left(\frac{\partial \bar{u}_0}{\partial \xi} + \frac{\delta}{r} \bar{u}_0 \right) f_1(\zeta) + \frac{\bar{u}_0}{r} \frac{\partial \bar{\psi}_0}{\partial \xi} f_1(\zeta) \right\}, \tag{22}$$

in which the overbars denote depth-averaging and the functions $f_1(\zeta), f_2(\zeta)$ are polynomials in ζ represented in figure 4. The depth-averaged quantities in (22) are given by

$$\bar{u}_0 = \frac{i_0}{3r}; \quad \bar{\psi}_0 = \frac{19}{2240} \bar{u}_0^2; \quad \bar{u}_1 = \frac{i_1}{3r} - \frac{3328}{7315} \left\{ 2 \frac{\bar{\psi}_0}{r} \left(\frac{\partial \bar{u}_0}{\partial \xi} + \frac{\delta}{r} \bar{u}_0 \right) + \frac{\bar{u}_0}{r} \frac{\partial \bar{\psi}_0}{\partial \xi} \right\}. \tag{23}$$

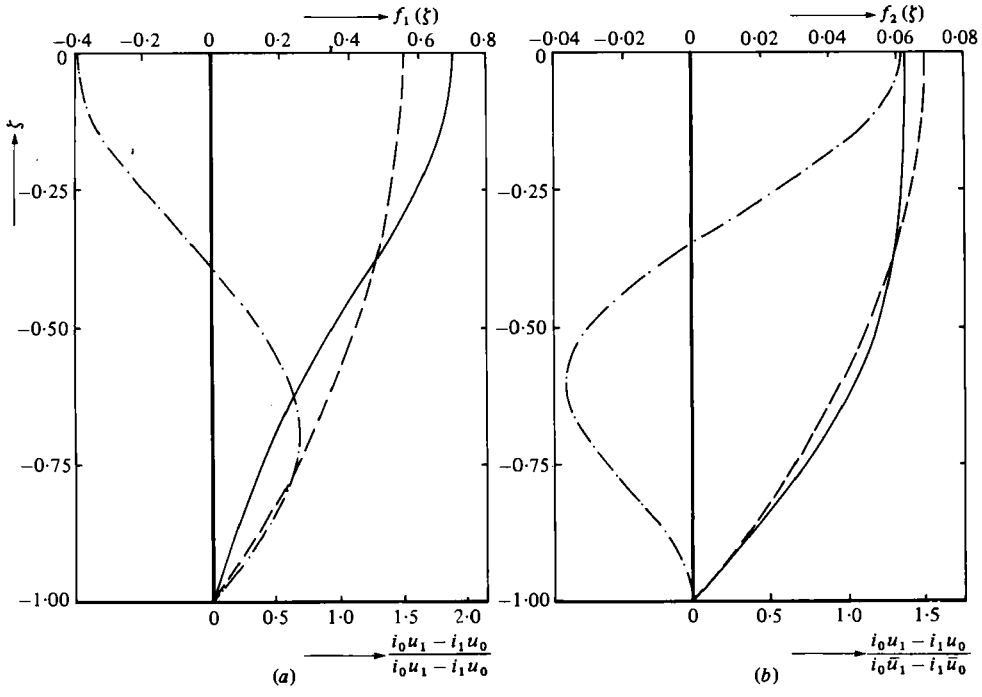

FIGURE 4. Low-Dean-number perturbations of the main velocity: (*a*) due to radial convection; (*b*) due to vertical convection (——, perturbation; – – –, parabola with the same depth-averaged value; —·—, perturbation function).

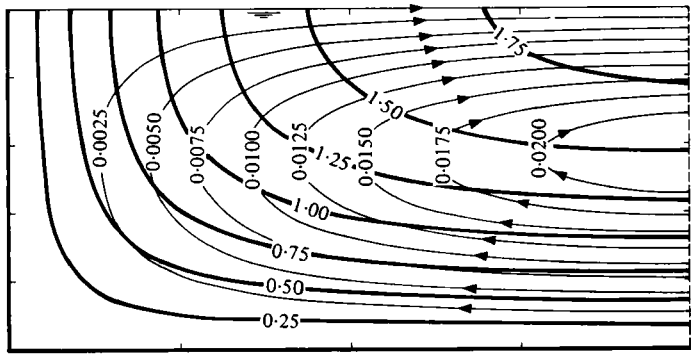

FIGURE 5. Main-flow isovels (——) and secondary-flow streamlines (——→) in the inner wall region of a shallow channel ($d/B = 0{\cdot}1$).

The contribution of the secondary-flow convection to $\bar{u}_1$ consists of two parts, due to the radial and the vertical velocity component, respectively. These two parts are negative near the inner wall and positive near the outer wall, whereas they almost vanish in the central part of the cross-section. Even though lateral diffusion is not negligible near the sidewalls, this readily shows the tendency of secondary-flow convection to reduce the depth-averaged main velocity near the inner wall and to increase it near the outer wall. Similarly, equation (22) and figure (4) show the radial velocity component to give rise to a flattening of the vertical distribution of u as long as $\partial\bar{u}_0/\partial\xi + \delta r^{-1}\bar{u}_0$ is relatively weak.

A physical interpretation of the foregoing can be given by considering the main-flow isovels and the streamlines of the secondary circulation for the zero-Dean-number limits u_0 and ψ_0, shown for the inner wall region in figure 5. Throughout the region shown in this figure u_0 increases along the streamlines of the secondary flow. This implies that everywhere in this region the fluid conveyed to a point by the secondary flow has a longitudinal momentum deficit with respect to the undisturbed flow in that point. As a consequence, an overall reduction of the main velocity with respect to u_0 occurs in the inner wall region. The opposite holds for the outer wall region, where the fluid conveyed by the secondary flow has a momentum surplus and the main velocity increases. The inclinations α_i and α_s of the isovels and the streamlines in figure 5 are given by

$$\tan\alpha_i = -\frac{\partial u_0}{\partial \xi}\Big/\frac{\partial u_0}{\partial \zeta} \quad \text{and} \quad \tan\alpha_s = -\frac{\partial \psi_0}{\partial \xi}\Big/\frac{\partial \psi_0}{\partial \zeta}, \tag{24}$$

whence it follows that

$$v_0\frac{\partial u_0}{\partial \xi} + w_0\frac{\partial u_0}{\partial \zeta} = [v_0^2+w_0^2]^{\frac{1}{2}}\left[\left(\frac{\partial u_0}{\partial \xi}\right)^2+\left(\frac{\partial u_0}{\partial \zeta}\right)^2\right]^{\frac{1}{2}}\sin(\alpha_s-\alpha_i). \tag{25}$$

Therefore, if the term $\delta r^{-1}u_0v_0$ is neglected,† the magnitude of the convection terms in the longitudinal momentum equation is proportional to the local intensity of the secondary flow, the local main velocity gradient and the sine of the angle of intersection between the main-flow isovels and the secondary-flow streamlines. According to figure 5, the streamlines and the isovels intersect at very small angles near the bottom, whereas they are almost perpendicular near the surface. The secondary-flow intensity is also somewhat smaller in the lower part of the cross-section and the main velocity gradient is of the same order of magnitude everywhere, at least close to the wall. Hence the convection terms will be largest in the upper part of the cross-section and the reduction of the velocity will be strongest there. Since the shape of the main velocity profile would not be affected if the sum of the convection terms were constant along a vertical line, this implies that the velocity profile becomes flatter near the surface.

The redistribution of the main velocity works out as a deformation of the main-flow isovels in the direction of the secondary flow. Essentially the same phenomenon is found in turbulent flow through straight non-circular conduits, where secondary circulations occur, as well. The deformation of the main-flow isovels can be explained in the same way as was done here (Prandtl 1952; see also Schlichting 1951; Reynolds 1974).

5. Analysis for intermediate-Dean-number flow

At small Dean numbers only small and local perturbations of the zero-Dean-number velocity occur, as was shown in § 4. As the Dean number increases, however, the perturbations grow stronger and lateral interaction grows more and more important, until the influence of secondary-flow convection is felt throughout the cross-section, whether this is shallow or not. The range of Dean numbers at which this lateral interaction process develops will be called intermediate. The upper bound of this range

† If this term, originating from the radial divergence of the co-ordinate system, is taken into account, the same reasoning holds for lines of constant ru_0 rather than for the isovels.

will be taken at the Dean number at which an additional longitudinal vortex starts to develop near the outer wall (cf. § 6).

The difference between the low and intermediate Dean-number ranges is reflected by the mathematical approach: the perturbation method described in § 4 applies no longer. The somewhat more crude similarity approximation

$$u(\xi,\zeta) = \bar{u}(\xi)\,F(\zeta), \quad \psi(\xi,\zeta) = \bar{\psi}(\xi)\,G(\zeta), \tag{26}$$

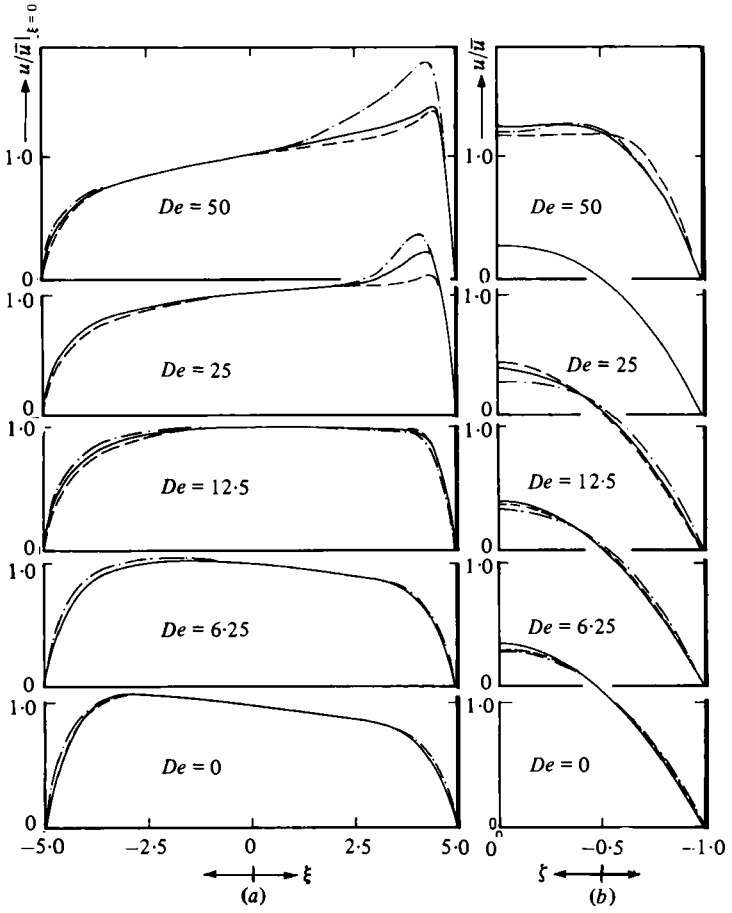

FIGURE 6. Similarity of the main velocity distribution for $\delta = 0{\cdot}04$ and $d/B = 0{\cdot}1$. (*a*) Vertical similarity (— —, $\zeta = -0{\cdot}9$; — · —, $\zeta = -0{\cdot}5$; - - -, $\zeta = 0$); (*b*) radial similarity (——, $\xi = 0$; — · —, $\xi = -4{\cdot}5$; - - -, $\xi = 4{\cdot}5$).

however, holds for the greater part of the cross-section at intermediate De as well (see figure 6). Hence the mathematical analyses of the horizontal and the vertical deformations of the main velocity distribution can be separated. The horizontal deformations are described by the depth-averaged longitudinal momentum equation

$$-De^2\overline{F\frac{\partial G}{\partial\zeta}}\frac{\bar{\psi}}{r}\frac{1}{r}\frac{\partial(r\bar{u})}{\partial\xi} + De^2\overline{G\frac{\partial F}{\partial\zeta}}\frac{\bar{u}}{r}\frac{\partial\bar{\psi}}{\partial\xi} = \delta\frac{i}{r} + \frac{\partial}{\partial\xi}\left\{\frac{1}{r}\frac{\partial(r\bar{u})}{\partial\xi}\right\} - \bar{u}\left.\frac{\partial F}{\partial\zeta}\right|_{\zeta=-1}, \tag{27}$$

in which the subsequent terms will be named radial convection term, vertical con-

vection term, longitudinal slope term, radial diffusion term and bottom shear stress term, respectively. If the solutions of F, G and $\overline{\psi}$ computed by the complete model are introduced as known functions, $\overline{u}$ and i are the only unknown quantities in (27). They can be solved from this equation, the integral condition of continuity (15) and the boundary conditions

$$\overline{u} = 0 \quad \text{at} \quad \xi = \pm \frac{B}{2d}. \tag{28}$$

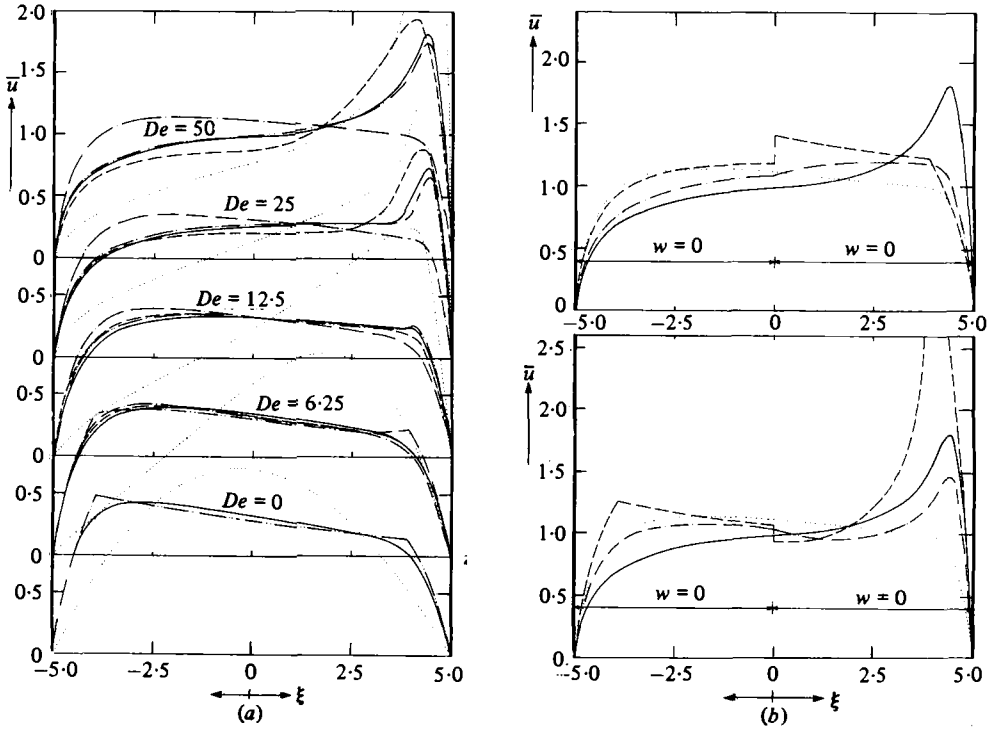

FIGURE 7. Analysis of the depth-averaged main velocity redistribution for $\delta = 0{\cdot}04$ and $d/B = 0{\cdot}1$. (*a*) Influence of secondary-flow convection, radial diffusion and bed shear stress (——, complete depth-averaged equation; — · —, vertical convection neglected; — —, radial convection neglected; — · · —, radial diffusion neglected for $-4 < \xi < 4$; . . . , bed shear stress neglected); (*b*) lateral interaction due to radial convection for $De = 50$ (——, complete depth-averaged equation; . . . , $w = 0$ for all ξ; – – –, $v = 0$ and — · —, $v \neq 0$ with radial diffusion neglected for $-4 > \xi > 4$ and $w = 0$ in the indicated region).

Figure 7 shows the influence of the convection, diffusion and bottom shear stress terms in equation (27). It gives rise to the following observations:

(i) if the vertical convection term is neglected, the depth-averaged velocity distribution hardly differs from its zero-Dean-number limit (see figure 7*a*);

(ii) if the lateral convection term is neglected, lateral interaction is almost absent, especially in the central region (see figure 7*b*);

(iii) the lateral interaction due to radial convection is exclusively outward (see figure 7*b*);

(iv) neglecting the radial diffusion term away from the side walls has hardly any influence on $\overline{u}$ (see figure 7*a*);

(v) neglecting the bottom shear stress gives rise to much less uniform and at higher De much more strongly skewed distributions of $\bar{u}$ (see figure 7*a*).

Hence it is concluded that the vertical convection term is the main cause of the local decrease of $\bar{u}$ near the inner wall and the local increase near the outer wall, whereas radial convection provides for an outward lateral interaction. Consequently, the region influenced by the local velocity reduction near the inner wall is extended outwards until it covers the greater part of the cross-section and the region influenced by the local velocity increase near the outer wall is compressed against the wall (see figure 7*a*, the influence of neglecting the radial convection term). If the bottom shear stress were absent, this combined effect of vertical and radial convection would lead to an almost linear increase of $\bar{u}$ with ξ in the central region. The bottom shear stress, however, tends to attenuate the non-uniformities. As a consequence, the distribution of $\bar{u}$ is deflected towards an almost horizontal asymptote.

A similar procedure can be followed to analyse the deformation of the vertical distribution function $F(\zeta)$, which is described by the longitudinal momentum equation

$$-De^2\frac{\bar{\psi}}{r^2}\frac{\partial(r\bar{u})}{\partial\xi}\frac{\partial G}{\partial\zeta}F'+De^2\frac{\bar{u}}{r}\frac{\partial\bar{\psi}}{\partial\xi}G\frac{\partial F'}{\partial\zeta}=1+\frac{\partial}{\partial\xi}\left\{\frac{1}{r}\frac{\partial(r\bar{u})}{\partial\xi}\right\}F'+\bar{u}\frac{\partial^2F'}{\partial\zeta^2}, \tag{29}$$

with $F=F'/\bar{F}'$ ($F=1$ by definition) and the boundary conditions

$$F'=0 \quad \text{at} \quad \zeta=-1, \quad \text{and} \quad \frac{\partial F'}{\partial\zeta}=0 \quad \text{at} \quad \zeta=0.$$

The subsequent terms in (29) will be referred to as the radial convection term, the vertical convection term, the longitudinal slope term, the radial diffusion term and the vertical diffusion term, respectively. The quantities G, $\bar{u}$ and $\bar{\psi}$ are derived from the complete model, so that F can be solved from the above system.

Figure 8 leads to the following conclusions as to the influence of the various terms in equation (29):

(i) in the inner wall region the vertical convection term causes a decrease of F near the bottom and an increase near the surface; the reverse occurs in the outer wall region;

(ii) the radial convection term acts in the opposite sense and its effect is considerably stronger, near the side walls and especially in the central region, where its influence on F is the same as near the inner wall;

(iii) the influence of radial diffusion and the no-slip conditions at the side walls is rather small.

As far as the side-wall regions are concerned, these observations qualitatively agree with the findings of § 4. In the central region, where F is hardly deformed at low Dean numbers, the flattening at higher De must obviously be attributed to radial convection.

The physical explanation of the local deformations of the main velocity distribution near the side walls is essentially the same as for low-Dean-number flow (§ 4). Away from the side walls the convective transport of momentum is mainly horizontal, outward in the upper half of the cross-section and inward in the lower half, such that there is a net outward momentum transport. With the bottom shear stress as a damping factor, this net outward transport gives rise to a retarded outward expansion of the low-velocity region near the inner wall. The velocity peak is compressed against the

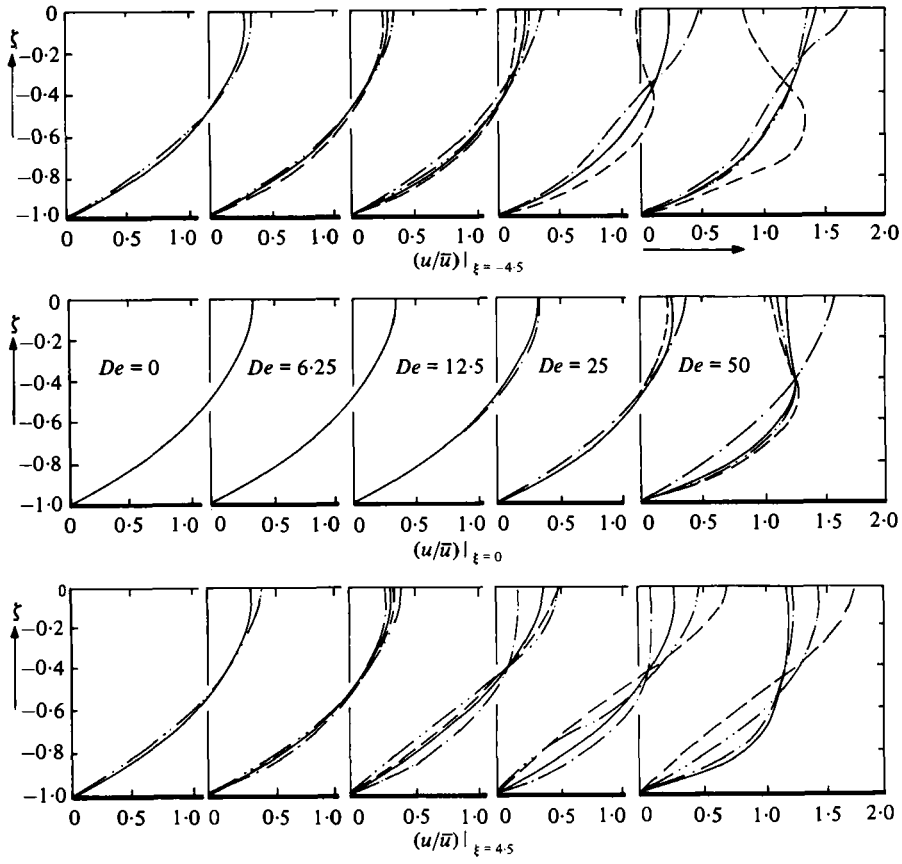

FIGURE 8. Analysis of the vertical distribution of the main velocity for $\delta = 0{\cdot}04$ and $d/B = 0{\cdot}1$ (——, complete vertical equation; – – –, vertical convection neglected; — · —, radial convection neglected; — · —, radial diffusion neglected).

outer wall, where it is partly damped by viscous forces. As a consequence, the main velocity distribution tends to be skewed outwards and hence radial convection causes a flattening of the vertical profile of u, the fluid conveyed from further inside giving rise to a momentum deficit in the upper half of the cross-section and the fluid conveyed from further outside causing a momentum surplus in the lower half (cf. § 4).

6. High-Dean-number flow

As was shown in § 2, the flow at effective Dean numbers (based on the mean turbulence viscosity instead of the molecular one) higher than 50 is not quite relevant to the mathematical modelling of the flow in river bends. Still there is one aspect of this flow that deserves some further attention, even from this river-engineering point of view.

If the Dean number is gradually raised from 50 to 60, a reverse secondary circulation suddenly develops near the surface in the outer wall region (cf. figure 9). Although the solution procedure in the present mathematical model becomes poorly convergent at Dean numbers higher than 60, other models, based on procedures that work well

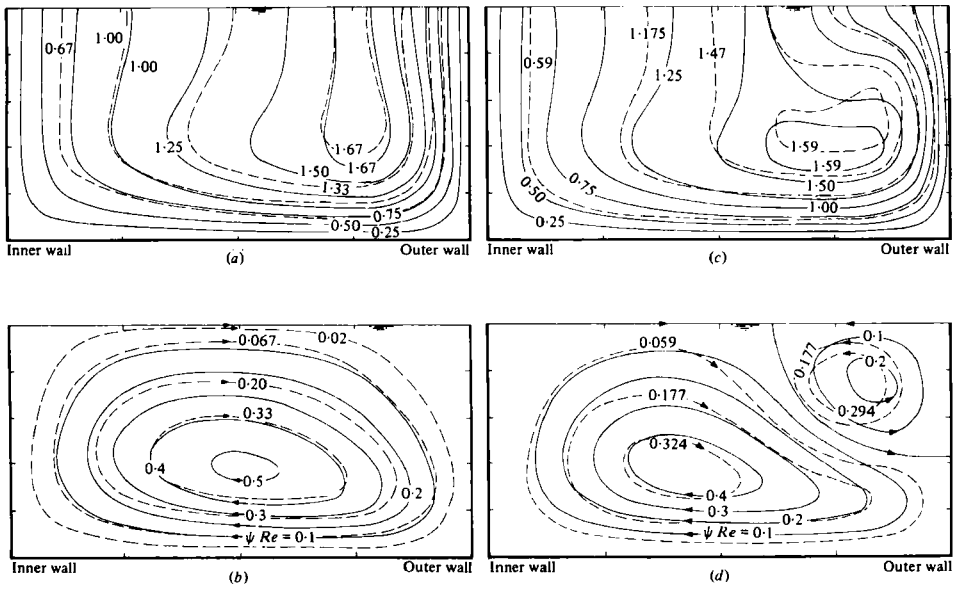

FIGURE 9. Transition from single to double helical flow pattern in a square pipe ($d/B = 0{\cdot}5$ and $\delta = 0{\cdot}1$; ——, present model; – – –, Joseph *et al.* (1975)). (*a*) Main-flow isovels at $De = 47{\cdot}4$; (*b*) streamlines of the secondary flow at $De = 47{\cdot}4$; (*c*) main-flow isovels at $De = 53{\cdot}8$; (*d*) streamlines of the secondary flow at $De = 53{\cdot}8$.

in this high-Dean-number range, have shown that this additional vortex is not spurious (Joseph *et al.* 1975; Cheng *et al.* 1976). Besides, a similar circulation was observed in several laboratory experiments on turbulent flow in curved channels, even at effective Dean numbers much smaller than 60 (Yen 1965; Rao 1975; Choudhary & Narasimhan 1977; De Vriend & Koch 1977; De Vriend 1979). This phenomenon seems to occur in natural rivers also (Bathurst, Thorne & Hey 1979). In these turbulent flows, however, the mechanism underlying this reverse secondary circulation is complicated by the effect of turbulence anisotropy near the concave bank. This anisotropy generates a streamwise vorticity of a similar kind as the vorticity of the additional secondary circulation meant here (see, for instance, Perkins 1970), thus enhancing the tendency of the secondary circulation to split up.

The reverse circulation is mostly restricted to the outer wall region (cf. Rao 1975), so that it is of no importance to the mathematical modelling of the flow in the other parts of the cross-section (see § 5). On the other hand, it influences the shear stress at the outer wall (bank) and hence it may be important to the meandering of natural rivers. Therefore it is worth while to try and find at least a qualitative explanation of this phenomenon. At the end of the intermediate-Dean-number range the main velocity maximum in a vertical lies below the surface (see § 5), so that the vertical derivative of u is negative near the surface. Consequently, the source term in the secondary-flow equation (10) is negative and hence the stream function ψ tends to become negative there, as well. As long as the main velocity shows an outward increase, the reverse secondary circulation corresponding to negative ψ will be attenuated: the momentum surplus caused by fluid convection from further outwards tends to make the velocity derivative and the source term in (10) positive, again. In the outer

wall region, however, the main velocity sharply decreases towards the wall. Hence the reverse circulation will intensify itself and its convective influence will give rise to a further reduction of the main velocity at the surface. This also explains the abruptness of the transition from the single-vortex to the double-vortex pattern: once the reverse circulation comes into existence near the outer wall, it intensifies itself as far as viscous forces permit.

The foregoing suggests that the development of the additional vortex is a matter of hydrodynamic instability. On closer investigation the underlying mechanism appears to be essentially the same as for the so-called Goertler vortices in the boundary layer along a concave wall (Görtler 1940; see also Schlichting 1951), for the instability of laminar flow in an infinitely deep narrow curved channel (Dean 1928*b*) and for the so-called Taylor vortices between two concentric rotating cylinders (Taylor 1923; see also Schlichting 1951). Each of these phenomena is characterized by a dimensionless number of the same nature as the Dean number.

7. Concluding remarks

Once again it should be stressed that the present analysis only has qualitative relevance to river flows. It gives an indication of how the secondary flow influences the main flow and what is important when incorporating this effect in a mathematical model of flow in curved shallow channels. It leads to the conclusion that the secondary circulation in curved channel flow can give rise to considerable deformations of the main velocity distribution at intermediate and high values of the Dean number. (Apart from that, these deformations are reflected in other phenomena, such as an overall increase of the boundary shear stress, often indicated as 'bend resistance'.) Another point that becomes evident from the foregoing is that the vertical velocity component, and hence the horizontal distribution of $\overline{\psi}$, must be properly represented in a mathematical model that is to describe the main velocity redistribution due to the secondary flow in a long bend. This is readily shown by the depth-averaged longitudinal momentum equation (27). It is the transverse variation of the convective transport $\overline{\psi}\overline{u}$ that figures in this equation, so an improper description of the transverse distribution of $\overline{\psi}$ has a direct influence on the longitudinal momentum distribution and hence on $\overline{u}$.

For rectangular channels and channels with a flat bottom and steeply sloping banks this implies that the side-wall regions, and especially the inner wall region, play an important role in the main velocity redistribution process, the greater part of the transverse variation of $\overline{\psi}$ being concentrated near the side walls. Consequently, mathematical models limited to the central region of shallow channels (Van Bendegom 1947; Engelund 1974; De Vriend 1976; Falcón 1979) will fail in these cases as soon as secondary-flow convection becomes important. Therefore verification of such models on the basis of laboratory experiments in rectangular channels, which is a rather common practice, should be avoided, unless the effective Dean number is small or the bends are so short and shallow that the influence of secondary flow convection has no opportunity to extend far from the side walls (in weakly meandering channels, for instance; see Gottlieb 1976).

In shallow channels with mildly sloping banks the side walls, if present at all, are much less important. Instead of being caused by the lateral diffusion in combination

with the no-slip conditions at the side walls, the transverse variations of the main velocity and the secondary flow are mainly due to the transverse variation of the depth of flow then. These variations are spread over a much wider region and allow for a mathematical model that disregards lateral diffusion and side-wall effects (Kalkwijk & De Vriend 1980). On the other hand, computations with such simplified models have made clear that, even in gently curved shallow channels with mildly sloping banks, a point bar in the inner part and a pool in the outer part of the bend, the influence of secondary flow convection can have a considerable effect on the main velocity distribution (Kalkwijk & De Vriend 1980).

The investigations reported herein are part of a research project on the flow and the bed topography in alluvial river bends, incorporated in the joint hydraulic research programme T.O.W. (Toegepast Onderzoek Waterstaat), in which Rijkswaterstaat, the Delft Hydraulics Laboratory and the Delft University of Technology participate.

REFERENCES

ADLER, M. 1934 Strömung in gekrümmten Rohren. *Z. angew. Math. Mech.* 257–275.

BATHURST, J. C., THORNE, C. R. & HEY, R. D. 1979 Secondary flow and shear stress at river bends. *Proc. A.S.C.E., J. Hydraulic Div.* **105** (HY10), 1277–1295.

BÖSS, P. 1938 In *Wasser- und Geschiebebewegung in gekrümmten Flusstrecken* (ed. H. Wittman & P. Böss). Springer.

BOUSSINESQ, J. 1868 Mémoire sur l'influence de frottement dans les mouvements réguliers des fluïdes. *J. Math. pures et appl.* (2ème série) **13**, 413–000.

CHENG, K. C. & AKIYAMA, M. 1970 Laminar forced convection heat transfer in curved rectangular channels. *Int. J. Heat Mass Transfer* **13**, 471–490.

CHENG, K. C., LIN, R.-C. & OU, J.-W. 1976 Fully developed laminar flow in curved rectangular channels. *Trans. A.S.M.E.* I, *J. Fluids Engng* **98**, 41–48.

CHOUDHARY, U. K. & NARASIMHAN, D. 1977 Flow in 180° open channel rigid boundary bends. *Proc. A.S.C.E., J. Hydraulic Div.* **103** (HY6), 651–657.

COLLINS, W. M. & DENNIS, S. C. R. 1975 The steady motion of a viscous fluid in a curved tube. *Quart. J. Mech. Appl. Math.* **28**, 133–156.

COLLINS, W. M. & DENNIS, S. C. R. 1976 Steady flow in a curved tube of triangular cross-section. *Proc. Roy. Soc.* A **352**, 189–211.

CUMING, H. G. 1952 The secondary flow in curved pipes. *Aero. Res. Center R. & M.* 2880.

DEAN, W. R. 1928*a* The stream-line motion of fluid in a curved pipe. *Phil. Mag.* S7, **5**, 673–695.

DEAN, W. R. 1928*b* Fluid motion in a curved channel. *Proc. Roy. Soc.* A **121**, 402–420.

DE VRIEND, H. J. 1973 Theory of viscous flow in curved shallow channels. *Comm. on Hydraulics, Delft Univ. of Techn., Rep.* 71–1. (Also: *Proc. Int. Symp. River Mech., Bankok*, 1973, paper A17.)

DE VRIEND, H. J. 1976 A mathematical model of steady flow in curved shallow channels. *Comm. on Hydraulics, Delft Univ. of Techn., Rep.* 76–1. (Also: *J. Hydraulic Res.* **15**, 1977, 37–54.)

DE VRIEND, H. J. 1978 Fully developed laminar flow in curved ducts. *Lab. Fluid Mech., Delft Univ. Tech., Int. rep.* 2–78.

DE VRIEND, H. J. 1979 Flow measurements in a curved rectangular channel. *Lab. Fluid Mech., Delft Univ. Tech., Int. rep.* 9–79.

DE VRIEND, H. J. & KOCH, F. G. 1977 Flow of water in a curved open channel with a fixed plane bed. *Delft Hydr. Lab., Delft Univ. of Tech., TOW-rep.* R657-VI/M1415-I.

EINSTEIN, H. A. & HARDER, J. A. 1954 Velocity distribution and boundary layer at channel bends. *Trans. Am. Geophys. Un.* **35**, 114–120.

ENGELUND, F. 1974 Flow and bed topography in channel bends. *Proc. A.S.C.E., J. Hydraulic Div.* **100** (HY11), 1631–1648.

FALCÓN, M. A. 1979 Analysis of flow in alluvial channel bends. Ph.D. thesis, Univ. of Iowa.

GÖRTLER, H. 1940 *Über eine dreidimensionale Instabilität laminarer Grenzschichten an konkaven Wänden.* Nachr. Wiss. Ges. Göttingen, Math. Phys. Klasse, Neue Folge 2, no. 1.

GOTTLIEB, L. 1976 Three-dimensional flow pattern and bed topography in meandering channels. *I.S.V.A., Techn. Univ. of Denmark, Series Paper* no. 11.

ITŌ, H. 1951 Theory on laminar flow through curved pipes of elliptic and rectangular cross-section. *Rep. Inst. High Speed Mech. Tohoku Univ.* **1**, 1–16.

JOSEPH, B., SMITH, E. P. & ADLER, R. J. 1975 Numerical treatment of laminar flow in helically coiled tubes of square cross-section; Part I – Stationary helically coiled tubes. *A.I.Ch.E. J.* **21**, 965–974.

KALKWIJK, J. P. TH. & DE VRIEND, H. J. 1980 Computation of the flow in shallow river bends. *J. Hydraulic Res.* **18**, no. 4.

KAMIYAMA, S. 1966 Two dimensional potential theory on flow through bend of arbitrary profile (Report 2). *Rep. Inst. High Speed Mech. Tohoku Univ.* **18**, no. 172, 25–42.

LEOPOLD, L. B., WOLMAN, M. G. & MILLER, J. P. 1964 *Fluvial Processes in Geomorphology.* San Francisco.

LESCHZINER, M. & RODI, W. 1978 Calculation of three-dimensional turbulent flow in strongly curved open channels. *Univ. Karlsruhe, Rep.* SFB80/T/126. (Also: *Proc. A.S.C.E., J. Hydraulic Div.* **105** (HY10), 1297–1315, 1979.)

MORI, Y., UCHIDA, U. & UKON, T. 1971 Forced convective heat transfer in a curved channel with a square cross-section. *Int. J. Heat Mass Transfer* **14**, 1787–1804.

MURAMOTO, Y. 1965 Flow through curved open channels, Part I – On characteristics of upper layer in fully developed region. *Bull. Dis. Prev. Res. Inst.* **14**, pt. 2, 1–14.

PATANKAR, S. V., PRATAP, V. S. & SPALDING, D. B. 1974 Prediction of laminar flow and heat transfer in helically coiled pipes. *J. Fluid Mech.* **62**, 539–551.

PATANKAR, S. V., PRATAP, V. S. & SPALDING, D. B. 1975 Prediction of turbulent flow in curved pipes. *J. Fluid Mech.* **67**, 583–595.

PERKINS, H. J. 1970 The formation of streamwise vorticity in turbulent flow. *J. Fluid Mech.* **44**, 721–740.

PRANDTL, L. 1952 *Essentials of Fluid Dynamics.* London: Blackie.

PRATAP, V. S. & SPALDING, D. B. 1975 Numerical computations of the flow in curved ducts. *Aero. Quart.* **26**, 219–228.

RAO, K. V. 1975 Secondary flow in a curved channel as revealed by a laser doppler anemometer. *Proc. LDA-Symp. Copenhagen*, pp. 710–718.

REYNOLDS, A. J. 1974 *Turbulent Flows in Engineering.* Wiley.

ROZOVSKII, I. L. 1961 *Flow of water in bends of open channels.* Israel Program for Scientific Translation, Jerusalem (in Russian, 1957).

SCHLICHTING, H. 1951 *Boundary Layer Theory.* Karlsruhe: Braun. (English edition: McGraw-Hill, 1968.)

TAYLOR, G. I. 1923 Stability of a viscous liquid contained between two rotating cylinders. *Phil. Trans. Roy. Soc.* A **223**, 289–343.

VAN BENDEGOM, L. 1947 Some considerations on river morphology and river improvement. *De Ingenieur* **59**, no. 4, B1–11 (in Dutch). Transl. 1963 *National Res. Council Canada, Techn. Transl.* no. 1054).

YEN, B. C. 1965 Characteristics of subcritical flow in a meandering channel. Inst. Hydr. Res., Univ. of Iowa.